

matrix is minor, and the contact force will dominate the development of G_0 . Thus, the change of soil fabric is mainly due to the change of suction stress during drying or wetting process. In this case, we exclude the influence on evolution of G_0 of boundary conditions. This desired loading/deformation condition capacitates the examination of effect of suction stress on the development of G_0 with respect to soil moisture.

3. EXPERIMENTAL PROGRAM

To test our hypothesis of the impact of suction stress on the G_0 evolution, experiments on 7 soils were conducted by incorporating shear-wave velocity measurement following the Drying Cake (DC) method (Lu and Kaya, 2013). FIG.2 shows an illustrative experimental setup of the shear-wave velocity measuring system using bender elements. The peripheral signal system for shear-wave measuring includes an oscilloscope with function generator module, a digital filter/amplifier. Signals were set up followed by Truong et al. (2011). A pair of bender elements was mounted at the center of the top and bottom surface of the soil cake. The transmitter sent a shear-wave through the soil cake and the vibration was detected by the receiver. The time of first arrival of shear-wave can be determined and shear-wave velocity is then calculated. The G_0 values can be calculated using $G_0 = \rho \cdot (V_s)^2$, where ρ is the unit mass density of soil, V_s is shear-wave velocity.

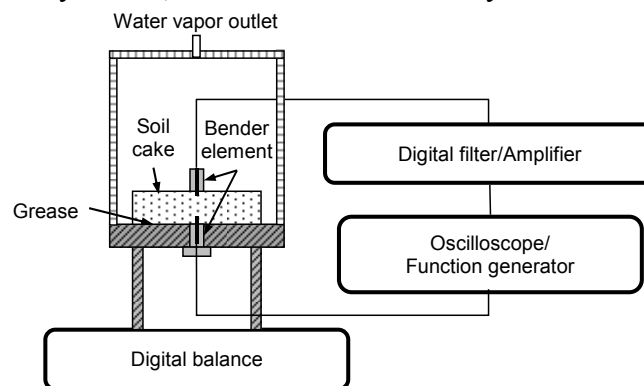


FIG.2 Schematic illustration of the soil cake specimen, sensors and signal system for small-wave velocity measurement using the Drying Cake method

The sample preparation procedure follows: first, soil cake specimens were compacted using a GeoJac loading frame; then samples were saturated by being immersed in water in a triaxial cell and applying vacuum for sufficient time (usually 1~2 days); last, using the loading frame again to consolidate the soil specimens. All soil cake specimens were prepared with 76.2 mm of diameter and ~20 mm of thickness. Then, soil cake specimens were placed on a plate with a thin layer of Vaseline grease to minimize the friction between soil and plate, so that the soil specimen has a zero boundary constraint and is free to deform. All soils were dried in a chamber with limited openings for lowering the evaporation rate. Thus, the reduced suction gradient between soil sample and surrounding air ensures the soil has homogeneous moisture distribution throughout the cake during the evaporation drying. The system was maintained at a constant room temperature and a relative humidity of ~10%, equivalent to a total suction of approximately 317 MPa according

to the Kelvin's equation (Lu and Likos, 2004). To monitor the weight change, the soil cake with the supporting plate was put on a digital balance for calculating degrees of saturation.

Another 5 soils from literature were added for validation. Those samples were tested using similar boundary conditions: no external loading and soils were air dried by natural evaporation. Table 1 lists all the soil properties (i.e., soil classifications, porosity) and the fitted parameters of VG model for measured SWRC of each soil.

Table 1 Properties and scaling factor of correlation for examined soils and fitting parameters of SWRC based on van Genuchten model

Soil #	Soil	USCS	ϕ	Van Genuchten model			A_0
				S_{res}	α	n	
1 *	Bonny silt	ML	0.47	0.11	0.097	1.44	0.0003
2 *	Hopi silt	SC	0.44	0.21	0.045	1.77	0.0011
3 *	BALT silt	ML	0.41	0.10	0.059	1.73	0.0008
4 *	Iowa silt	ML	0.49	0.20	0.082	1.56	0.0007
5 *	Denver claystone	CL	0.51	0.16	0.011	1.47	0.0026
6 *	Denver Bentonite	CH	0.69	0.36	0.014	1.38	0.0046
7 *	Missouri clay	CL	0.41	0.25	0.023	1.45	0.0004
8 #	S1	MH	0.50	0.04	0.006	1.90	0.0050
9 #	S2	MH	0.56	0.01	0.006	1.87	0.0144
10 #	S3	MH	0.56	0.01	0.007	1.72	0.0107
11 #	S4	MH	0.54	0.01	0.007	1.79	0.0075
12 #	S5	MH	0.56	0.01	0.004	1.86	0.0175

References: * from this study, # SWRC and G_0 data from Mendoza et al. (2006)

4. COMPARISONS OF G_0 AND SUCTION STRESS

Fig. 3 and 4 show the measured SWRCs fitted using VG model in terms of degree of saturation in kPa, and calculated SSCCs in -kPa. The experimental G_0 data points with degree of saturation in MPa are also plotted. Fig. 3 presents the results of experiment measurements conducted in this study, and Fig. 4 replots the results from Mendoza et al. (2006) for the validation. The fitted residual soil moistures are calculated in terms of degree of saturation. The type of soil tested in this paper varies from sandy silt (Hopi silt) to clayey soil (Denver bentonite). The residual soil moistures range of 0.10 to 0.36 degrees of saturation. The highest suction stress developed during drying process can reach from ~50 kPa (Hopi silt) to over 5000 kPa (Denver claystone) when the degree of saturation is approaching to the residual soil moisture. The other 5 soils from the literature have much less residual soil water than soils tested in this paper, and some soil samples did not start drying from fully saturated condition (S2-S5).

The measured G_0 in Fig. 3 covers a wide range of degrees of saturation, due to the low relative humidity in the room condition. The ~10% relative humidity, or over 300 kPa matric suction equivalent, dries the soil specimens cross the capillary water regime and cover part of the adsorption water regime. Considering the limited capability of VG model of SWRC, matric suction of soil close to the residual degree of saturation is not reliable and suction in the adsorption water regime below the residual degree of saturation is not available. And suction stress of unsaturated soils at such range of soil moisture is not well defined. Therefore, the comparison between G_0 and suction stress will be focused on only in capillary water regime.

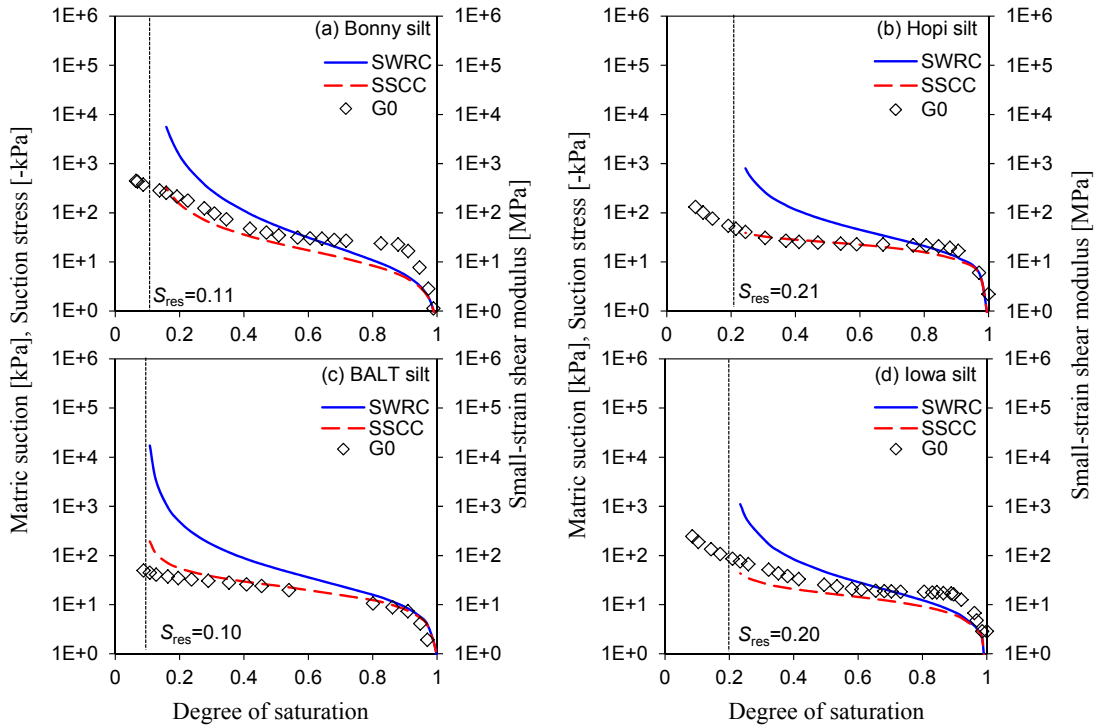


FIG.3 Comparison of SWRC and SSCC using van Genuchten model and the measured small-strain shear modulus using the Drying Cake method

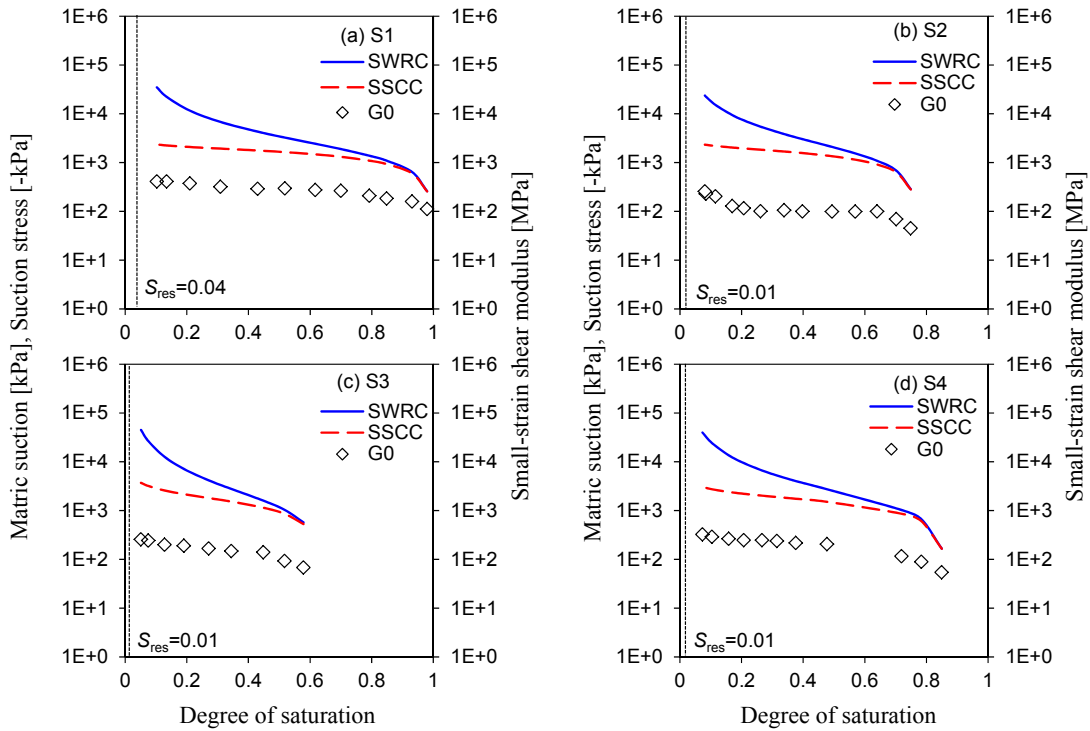


FIG.4 Comparison of SWRC and SSCC using van Genuchten model and the measured G₀ from Mendoza et al. (2006)

From both Fig. 3 and 4, we can observe that G_0 increases with the decreasing degree of saturation as the soil dries, in a very similar pattern as the suction stress develops. G_0 captures well for the initial increase in the capillary fringe before the air entry. When soils start to desaturate, G_0 gradually increases proportional to the suction stress increment. G_0 continues to develop along the similar path with suction stress until the degree of saturation is close to the residual soil moisture. The overall behavior of the G_0 evolution significantly resembles the SSCC in the capillary soil water regime.

Fig. 5 shows the comparison of measured G_0 and the calculated suction stress for saturation higher than S_{res} . G_0 increases as suction stress increasing. A considerably high linearity can be found from the results for all soils. Except the 0.67 for S2 soil, the coefficients of correlation for G_0 and SSCC range from 0.91 to 0.99. In other word, the suction stress differs with G_0 only by a multiplying scaler. This observation reflects that the conceptualized inter-particle force term, suction stress, is well manifested by the indicator of contact force of soil skeleton, G_0 . It also illustrates that the small-strain stiffness is mainly contributed by the inter-particle stress at the contacts, rather than the change of the modulus of the material.

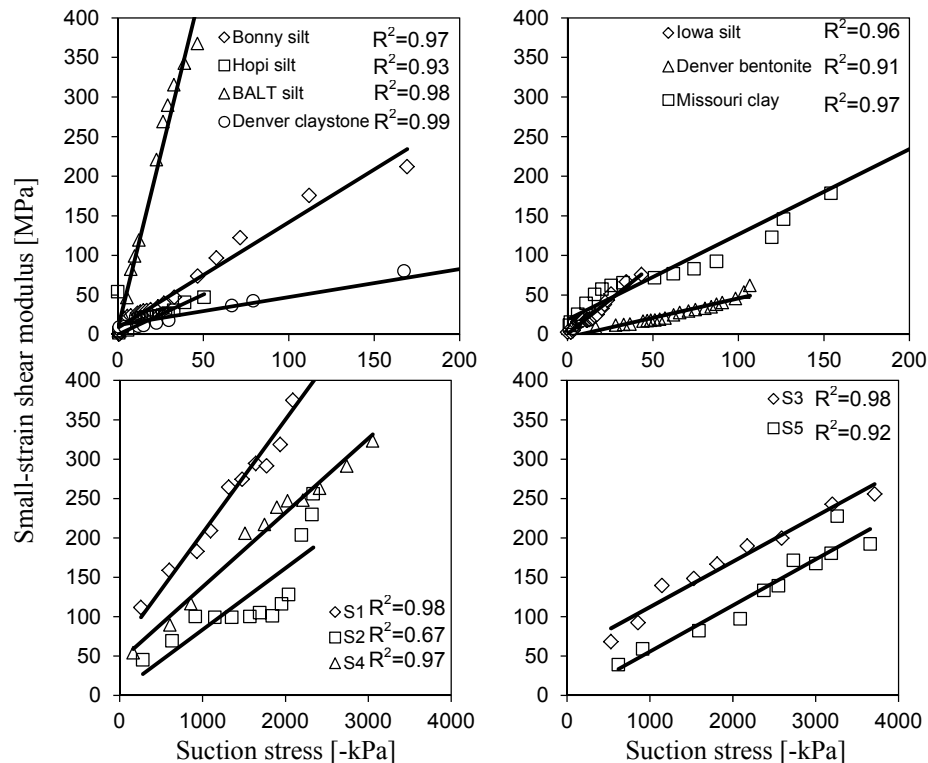


FIG.5 Comparison of experimental data of G_0 with SSCC

Based on the high linearity between G_0 and suction stress, a simple equation can be proposed to express the correlation between these two:

$$\sigma^s = A_0 \cdot G_0 \quad (5)$$

where A_0 is dimensionless scaler depended on soil types. The values of A_0 are also listed in Table 1, varying from number 0.00003 up to 0.0175. Then, a correlation between A_0 and the SWRC parameter α of VG model, the inverse of air-entry suction, is presented in Fig. 6. Parameter α represents the largest pore size. For soils with

higher α value, or lower air-entry pressure, the correlation between G_0 and SSCC has lower A_0 value. The scaler A_0 decays with the increase of α in an exponential way, which can be empirical determined by fitting the data points in Fig 6, in equation form: $A_0 = (9 \cdot 10^{-6}) \alpha^{-1.32}$.

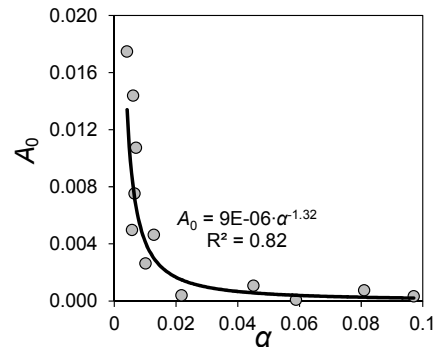


FIG.6 Comparison of experimental data of G_0 with SSCC

5. CONCLUSIONS

We discussed about the G_0 evolution as the degree of saturation changing for unsaturated soils using suction stress theory as the effective stress framework. The experimental measurements were conducted on the soil cake samples under intentionally specified conditions: zero external loading and no displacement constraints during controlled evaporation drying process. This free boundary condition is in effect to exclude the impact on soil fabric change induced by external loading and unnecessary deformations. Therefore, the only force taking the role is the inter-particle contact force, suction stress. The experimental data conducted in this study and collected from literature are used to verify the hypothesis. SWRC model of van Genuchten is used to express the soil water retention behavior for each soil. The residual degrees of saturation are identified to differentiate the capillary and adsorption regime for soil water distribution. The well-established suction stress in capillary regime is compared with the development of G_0 as degree of saturation changes. Similar evolving pattern with saturation was found for both SSCC and G_0 . A high linearity between G_0 and SSCC can be defined by a dimensionless scaler A_0 . A strong correlation between A_0 and SWRC parameter α is determined by an empirical fitting. By examining the G_0 development, this inherent connection verifies the validity of the suction stress as effective stress principle, and its capability of describing the inter-particle force and the contact behavior for unsaturated soils.

ACKNOWLEDGEMENTS

This research is supported by grant from the National Science Foundation (NSF CMMI-1230544) to NL.

REFERENCES

Bishop, A.W. (1959). "The principle of effective stress." *Teknisk Ukeblad I Samarbeide Med Teknikk*, 106(39), 859–863.

- Clayton, C.R.I. (2011). "Stiffness at small strain: research and practice." *Géotechnique*, 61(1) 5–37.
- Cho, G.C., and Santamarina, J.C. (2001). "Unsaturated particulate materials: particle-level studies." *J. Geotech. Geoenviron. Eng.* 127(1), 84–96.
- Dong, Y., Lu, N., and McCartney, J.S. (2015). "A Unified Model for Small-Strain Shear Modulus of Variably Saturated Soil." *J. Geotech. Geoenviron. Eng.*
- Hardin B.O., and Richart F.E. (1963). "Elastic wave velocities in granular soils." *Journal of Soil Mechanics and Foundations Division ASCE*, 89(1), 33–65.
- Hardin B.O., and Drnevich V.P. (1972). "Shear modulus and damping in soils: design equations and curves" *Journal of Soil Mechanics and Foundations Division ASCE*, 98: SM 6-7.
- Heitor A., Indraratna B., and Rujikiatkamjorn C. (2013). "Laboratory study of small-strain behavior of a compacted silty sand." *Can. Geotech. J.*, 50(2), 179–188.
- Khosravi, A., and McCartney, J.S. (2012). "Impact of hydraulic hysteresis on the small-strain shear modulus of low plasticity soils." *J. Geotech. Geoenviron. Eng.*, 138(11), 1326–1333.
- Lu, N., Godt, J., and Wu, D. (2010). "A closed form equation for effective stress in variably saturated soil." *Water Resour. Res.*, 46(5), W05515.
- Lu, N., and Kaya, M. (2013). "A drying cake method for measuring suction-stress characteristic curve, soil-water-retention curve, and hydraulic conductivity function." *Geotech. Test. J.*, 36(1), 1–19.
- Lu, N., and Kaya, M. (2014). "Power law for elastic moduli of unsaturated soil." *J. Geotech. Geoenviron. Eng.*, 140, 46–56.
- Lu, N., and Likos, W.J. (2004). *Unsaturated soil mechanics*, Wiley, Hoboken, NJ.
- Lu, N., and Likos, W.J. (2006). "Suction stress characteristic curve for unsaturated soils." *J. Geotech. Geoenviron. Eng.*, 132(2), 131–142.
- Mendoza, C.E., Colmenares, J.E., and Merchán, V.E., (2005), "Stiffness of an unsaturated compacted clayey soil at very small strains." In: *Proceedings of international symposium on advanced experimental unsaturated soil mechanics*, 27–29 June, Trento, Italy, pp 199–204.
- Oh, W.T., and Vanapalli, S.K., (2014). "Semi-empirical model for estimating the small-strain shear modulus of unsaturated non-plastic sandy soils." *Geotech. Geol. Eng.*, 32, 259–271.
- Santamarina, J.C., Klein, K.A., and Fam, M.A. (2001). *Soils and Waves: Particulate Materials Behavior, Characterization and Process Monitoring*, Wiley, Chichester, U.K.
- Sawangsurriya, A., Edil, T. B., and Bosscher, P. J. (2009). "Modulus-suction moisture relationship for compacted soils in post compaction state." *J. Geotech. Geoenviron. Eng.*, 135(10), 1390–1403.
- Truong, Q., Lee, J., Dong, Y., and Yun, T. (2011). "Capillary induced small-strain stiffness for hydrophilic and hydrophobic granular materials: Experimental and numerical studies." *Soils and Foundations*, 51(4), 713–721.
- van Genuchten, M.T. (1980). "A closed-form equation for predicting the hydraulic conductivity of unsaturated soils." *Soil Sci. Soc. Am. J.*, 44(5), 892–898.
- Yang, J. and Gu, X.Q. (2013). "Shear stiffness of granular material at small strains: does it depend on grain size?" *Géotechnique*, 63(2), 165–179.

The Development and Evaluation of a Time Domain Reflectometry Probe for Soil Moisture and Suction Measurement

Xinbao Yu¹; Nan Zhang, M.ASCE, P.E.²; and Anand J. Puppala, F.ASCE, P.E.³

¹Assistant Professor, Dept. of Civil Engineering, Univ. of Texas at Arlington, 701 S. Nedderman Dr., Arlington, TX 76019. E-mail: xinbao@uta.edu

²Postdoctoral Researcher, Dept. of Civil Engineering, Univ. of Texas at Arlington, Arlington, 701 S. Nedderman Dr., TX 76019. E-mail: nan.zhang@mavs.uta.edu

³Professor, Dept. of Civil Engineering, Univ. of Texas at Arlington, 701 S. Nedderman Dr, Arlington, TX 76019. E-mail: anand@uta.edu

Abstract: Soil moisture and suction are two key variables that often need to be measured for unsaturated soil. They are commonly measured by separate soil moisture and suction sensors which require double installation efforts and often result in questionable correlation between the measured moisture and suction. Attempts were made to combine time domain reflectometry (TDR) and porous blocks functioning as tensiometers and have demonstrated a great potential of the TDR for simultaneous measurements of soil moisture and suction. In this study, a new TDR moisture-suction probe is designed based on the previous study, and it was evaluated in laboratory for simultaneous measurements of moisture content and soil suction. The probe has two parts with one half portion embedded in a dental plaster (i.e. gypsum) for soil suction measurements, whose suction is equilibrated with the surrounding soils. The other half portion of the probe is also inserted into the soils to measure moisture content. The probe calibration was completed by the use of pressure plate tests to establish a relationship between suction (ψ) and measured dielectric constant (K_a) of the gypsum block. Then, it was tested in a silty sand to evaluate its function for soil moisture and suction measurement. The preliminary test results demonstrated that the change of K_a of the gypsum corresponded well to suction level from 10 to 750 kPa, and it can measure moisture content and soil suction accurately for the test soils. The new probe can be fabricated easily and fast, without any additional maintenance and has a great potential for field measurement of soil moisture and suction.

INTRODUCTION

Soil water characteristic curve (SWCC) defines the relationship between volumetric water content and soil suction, which is important to characterize the behavior of unsaturated soils. It can be obtained in the laboratory by several commonly used methods such as filter paper, pressure plate extractor, and tempe pressure cell.

Determination of SWCC curves in the field still remains challenging due to the limitation of existing measurement sensors. Soil matric suction is often measured by a tensiometer limited to a measure range 0 to 85 kPa (Cassel and Klute, 1986). Thermocouple psychrometry can be used to measure matric suction in a wide range but it is very sensitive to temperature changes (Rawlins and Campbell, 1986). Noborio et al. (1999) demonstrated the use of a constructed porous medium to measure soil matric suction indirectly based on the measured moisture content, thermal, or electrical properties of the porous medium at equilibrium with the surrounding soils. A correlation of the measured property with matric suction for the used medium should be established before the measurement. For specific range of water potential, heat dissipation method, filter paper method, or gypsum block electrical-resistance method may be used in laboratory and in the field (Campbell et al., 1986).

Time domain reflectometry (TDR) technique has been demonstrated successfully to measure soil moisture content both in laboratory and in the field (Yu and Drnevich, 2004, Zhang, 2015). Baumgartner et al. (1994) and Whalley et al. (1994) attached porous materials functioning as tensiometers to the end of hollow electrodes of the TDR probe for simultaneous measurements of soil moisture content and matric suction. But the same limitation as the tensiometer does exist, which is the need to supply water to tensiometers and the limited measuring range of 0 to 85 kPa.

This paper presents the design and evaluation of a new moisture-suction TDR probe for simultaneous measurement of soil moisture and suction. Design and fabrication of the probe is first introduced. Then, the calibration of the probe is obtained by the use of pressure plate test to establish the relationship between matric suction and dielectric constant (K_a) of a gypsum block. The probe is also evaluated through laboratory experiments on a silty sand, and validated against the tempe pressure cell method.

PROBE DESIGN AND FABRICATION

The impedance of a TDR probe is a function of the probe spacing and diameter in addition to the dielectric constant of the test medium. A change of impedance within a probe due to the change of probe spacing or diameter can be detected in the recorded TDR waveforms (Davis, 1975). Knight (1992) and Petersen et al. (1995) suggested that a ratio of probe spacing to probe diameter should not be greater than 10 to avoid concentrating the sensing volume around the rods. Petersen et al. (1995) also indicated that the distance between TDR probe and the surface should be greater than 10, 15 and 20 mm for probes with spacing of 10, 20 and 50 mm, respectively, in order to avoid effects of incidents occurring on or near the soil surface on TDR measurement. Moreover, the distance between the probe in the gypsum and the nearest gypsum surface is 10 mm, which is large enough to involve all the electromagnetic energy as suggested by Petersen et al. (1995). Consequently, the design of the probe can satisfy the main design criteria based on the previous studies.

Based on the above design constraints, a moisture-suction TDR probe is designed to have two parts: upper and lower as shown Figure 1. The upper part consists of two stainless steel rods with diameter of 2 mm and spacing of 25 mm and it is used to

measure soil moisture; the lower part consists of two rods with the same diameter but smaller spacing of 5 mm embedded in a gypsum block (25 mm×25 mm×50 mm) and is used to measure soil suction. It is noted that the probe geometry change is used to amplify the impedance contrast between the upper and lower part for accurate reflection detection at the interface of the two parts.

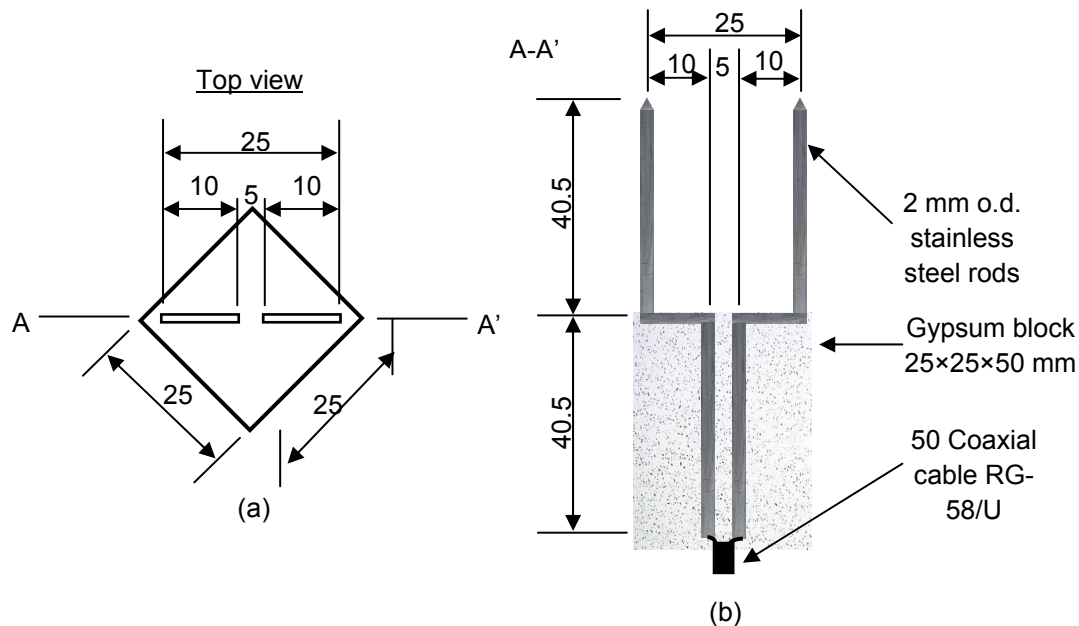


FIG. 1. Schematic of moisture-suction TDR probe: (a) top view, (b) side view (unit: mm).

According to the above design, the fabrication of the probe is described as follows: (1) Two stainless rods with diameters of 2 mm and length of 91 mm were bended in the shape as shown in Figure 1. The pointed tip was also made at the end of the rods to avoid soil disturbance as much as possible during the insertion process; (2) The two rods were then clamped and placed in the center of a prefabricated teflon mold; (3) A teflon spacer was used to clamp the rods outside the mold to fix the rod spacing (i.e. $s=25$ mm); (4) The inner and outer wires of a coaxial cable was connected to the top ends of the rods by soldering. (5) The lab plaster was mixed with tap water in a ratio of 30 mL of water to 50 g of the lab plaster. The slurry of the lab plaster was then poured into the teflon mold. The slurry was also stirred in the mold by a thin steel rod to remove the air bubbles as much as possible; (6) The teflon mold and spacer were removed after 24 h, and the moisture-suction TDR probe was completed as shown in Figure 2; (7) The probe was left under room temperature (23-24 °C) for several days until the solidification process inside the gypsum block was completed.

PROBE CALIBRATION FOR SUCTION MEASUREMENT

The pressure plate test was employed to obtain the calibration relationship between ψ and K_a of the gypsum block. The test procedures are as follows: (1) the gypsum block along with the rods and the ceramic plate with air entry value of 15 bar were saturated in tap water for 24 h according to ASTM standard D6836; (2) The weight of

saturated gypsum block was first measured, and it was then transferred into the pressure plate chamber as shown in Figure 3; (3) A burette was connected to the chamber by an outflow tube to measure the volume change of water in the gypsum block; (4) The air pressure of 7.5 bar was applied into the chamber and the volume change of water was monitored every day; (5) The outflow tube was removed firstly when the volume change of water is less than one line per day, and the air supply was then closed; (6) The chamber was opened, the probe was taken out and the weight of gypsum block was measured again; (7) The coaxial cable was then connected to Campbell Scientific TDR 100 to collect the TDR waveforms with the rods exposed in air; (8) Above test procedures were repeated under other air pressures, i.e. 4.0, 2.0, 1.0, 0.8, 0.5, 0.3, 0.1 bar.



FIG. 2. Photo of the moisture-suction TDR probe.

The dielectric constant of gypsum block and soils were determined (Baker and Allmaras, 1990) by,

$$K_{a,g} = (L_{a,g} / L)^2 \quad (1)$$

$$K_{a,s} = (L_{a,s} / L)^2 \quad (2)$$

where $K_{a,g}$ and $K_{a,s}$ are the dielectric constant of gypsum block and soils, respectively; $L_{a,g}$ is the apparent length of gypsum block, which is the distance between the first and the second reflection points in TDR waveforms; $L_{a,s}$ is the apparent length of soils, which is the distance between the second and the third reflections point in TDR waveforms; L is the length of the rod, i.e. 0.0405 m.

Figure 4 indicates the reflected TDR waveforms and the derivatives of the probe after the pressure plate test. The symbol “Saturated” refers to the saturated gypsum block before the pressure plate test. The local peak value of the derivatives directly indicates the reflection point of TDR waveforms. It is evident that both the waveforms and the second reflection point were shifting to the right as suction decreased, but the first reflection point remained at the same location. As a result, the $K_{a,g}$ was increased based on Eq. 1. This is because the higher suction will cause more moisture loss of the gypsum block in pressure plate test.